OBJECT IMAGING WITH A PIEZOELECTRIC ROBOTIC TACTILE SENSOR

Craig S. Dyson, Capt, USAF
Nik C. Yauilla
Edward S. Kolesar, Jr., PhD, P.E., Lt Col, USAF

Air Force Institute of Technology
Department of Electrical and Computer Engineering
Wright-Patterson AFB, Dayton, OH 45433-6583

ABSTRACT

A two-dimensional, electrically-multiplexed robotic tactile sensor was realized by coupling a piezoelectric polyvinylidene fluoride (PVDF) polymer film to a monolithic silicon integrated circuit (IC). The IC incorporates 64 sensor electrodes arranged in a symmetrical 8 x 8 matrix. Each electrode occupies a 400 x 400 μm square area, and they are separated from each other by 300 μm. A 40-μm thick piezoelectric PVDF polymer film was attached to the electrode array with an electrically non-conductive urethane adhesive. The response of the tactile sensor is linear for loads spanning 0.8 to 135 grams of force (gmf). The response bandwidth is 25 Hz, the hysteresis level is tolerable, and, for operation in the sensor's linear range, taxel crosstalk is negligible. The historically persistent stability and response reproducibility limitation associated with piezoelectric-based tactile sensors has been solved by implementing a novel pre-charge voltage bias technique to initialize the pre- and post-load sensor responses. A rudimentary tactile object image measurement procedure for applied loads has been devised to recognize the silhouette of a sharp edge, square, trapezoid, isosceles triangle, circle, toroid, slotted screw, and cross-slotted screw.

INTRODUCTION

The accomplishment of complex and delicate manipulative tasks in the industrial manufacturing setting will require future robots to possess sensory capabilities that are functionally equivalent to the human senses, the most critical being vision and touch. Without the equivalency of these two fundamental senses, robots will not be able to autonomously interact with a dynamic environment, and their evolution will likely be limited to the repetitious execution of a set of precisely programmed operations necessary to accomplish a dedicated task [1-5].

The sense of touch is of particular importance to autonomous robots, although it has not been as comprehensively investigated as vision sensing [6-8]. While vision is essential for range finding, identifying objects, and avoiding obstacles, the accomplishment of intricate manipulative manufacturing tasks will require a robot to first, grasp an object without damaging it, and second, to determine its physical characteristics (for example, weight, shape, orientation, hardness, texture, and temperature) [1,3-5,8]. Collectively, this complex physical sensing mode is referred to as taction [9-12]. Hence, the ideal tactile sensor will not only detect an object's morphology, it will also determine the amount of force and torque required to grasp it without slippage during manipulation.

The technological solution to the tactile sensing problem will likely involve gripper-mounted sensors composed of two-dimensional arrays of closely-spaced force sensing elements (taxels) which are linked to a computer dedicated to the tasks of gathering and interpreting the sensor's data to develop a tactile image of a grasped object. It is conceivable that, with rapid and repetitious sensor scans, the processed information will be sufficiently precise to be useful for controlling the grasp and manipulation of an object, thereby expanding the functionality and autonomy of a robot.

The thrust of the emerging tactile sensor research is to quantitatively measure contact forces (or pressures), mimic human-like spatial resolution and sensitivity, operate with a large bandwidth (fast response), and possess a linearizable response without manifesting significant hysteresis. To be successful in this endeavor, a general-purpose robotic manipulator (gripper) tactile sensor, in addition to being cost-effective, compliant (conformable to irregular surfaces) and physically robust, is envisaged to possess the following characteristics [1,3,5,8]:

1. A limited number of sensor elements (taxels) to minimize tactile image processing time; typical estimates range in number from 25 (5 x 5) to 256 (16 x 16).
2. Spacing of taxels to mimic the human two-point limen (threshold) of 1 mm center-to-center.
3. Sensitive to forces spanning 1 gram (interpreted as 1 gmf or 0.01 N) to 1000 grams (1000 gmf or 10 N); an incremental force resolution of 1 gram is desirable.
4. Discrete taxel response bandwidth of 100 Hz; it is recognized that this capability will be under utilized on a time-averaged basis.
5. Reasonable response linearity; some nonlinearity accepted provided computational resources can be devoted to compensate for it.
6. Negligible hysteresis is desired; however, a known transfer function can be compensated for computationally.

Toward the goal of enhancing the tactile performance of robots, several technologies are aggressively being investigated. Excluding the simple contact or switching technologies [1,4-5], which only yield one bit of information, the veritable tactile sensor technologies can be categorized to include: optical [1-5,13], (chemico-, mechano-, and piezo-) resistive [1-5,14], capacitive [3-5,15], inductive [4,5,16], piezoelectric [1,3-5,14,15,17], and acoustic [1,4,5,18].

The functionality of piezoelectric-based tactile sensors can be attributed to the well-established piezoelectric effect which predicts that the surface charge in a piezoelectric material is produced upon the application of an external force. The finite surface charge (Q) that is produced is proportional to the applied force (F) via the relation, $Q = SF$, where S is the charge sensitivity constant of the piezoelectric material [1,4,5]. By utilizing the piezoelectric material as the dielectric medium in a parallel plate capacitor configuration, the ideal (assuming a lossless dielectric and ignoring edge effects) capacitance (C) is given by

$$C = \frac{\varepsilon_0 \varepsilon_r A}{d} \qquad (1)$$

where A is the electrode's surface area, d is the dielectric's thickness, ε_o is the permittivity of free space, and ε_r is the relative dielectric constant collinear with the direction of the applied force (ε_r = 11 for PVDF) [19]. Thus, by invoking Gauss Law, the open-circuit voltage (V) generated at the capacitor's terminals is given by

$$V = \frac{Q}{C} = \left(\frac{S}{C}\right) F \quad . \qquad (2)$$

This paper reports the progress achieved toward realizing an adult fingertip-sized tactile sensor which has resulted from the direct coupling of a piezoelectric PVDF polymer thin film to an electrode matrix realized on a silicon integrated circuit (IC). To minimize electrical noise and impedance mismatch effects, a two-dimensional matrix of *in situ* high-input impedance metal-oxide-semiconductor field-effect transistor (MOSFET) amplifiers have been directly gate-contact coupled to the lower surface of the piezoelectric PVDF polymer film. This *in situ* MOSFET amplifier arrangement provides a separate, but identical, high-input impedance (10^{12} Ω) voltage measurement capability for each taxel. Short length electrical conductors were also judiciously utilized to minimize the coupling capacitance between taxel conductors. Since the MOSFET amplifiers isolate the PVDF film, have a low output impedance, and amplify the taxel's response to an acceptable signal level without seriously reducing the piezoelectric material's discharge characteristic, external discrete ICs (Maxim Integrated Products, model MAX328CPE, Sunnyvale, CA 94086) were used to implement an electronic multiplexer which is capable of scanning the 8 x 8 taxel matrix in 50 milliseconds (ms). Because response stability and reproducibility has historically limited the utility of piezoelectric-based tactile sensors [1,3-5,14,15,17], a solution to this problem has been devised and implemented [20]. That is, between each tactile object image measurement, a pre-charge stabilization bias was incorporated into the sensor's design and operation by providing external circuitry which is used to impress a short-duration (0.1 second), low-level, direct current voltage (V_{bias} = 2.5 V) to the upper and lower electrodes of the PVDF film. This pre-charge feature minimizes the voltage fluctuations observed between applications of an external load, and it subsequently manifests its benefit in the formation of an object's tactile image.

TACTILE SENSOR DESIGN

To realize a tactile sensor no larger than an adult's fingertip, a silicon IC with peripheral dimensions of 9200 x 7900 μm was designed and fabricated using the Metal-Oxide-Semiconductor Implementation System's (MOSIS) 2-μm, n-well, two-level metal, complementary metal-oxide-semiconductor (CMOS) technology [21]. After a portion of the IC's area was reserved for the MOSFET amplification and output interface circuitry, the 8 x 8 taxel matrix was allocated to a 5300 x 5300 μm area such that the sensor's ideal spatial resolution was somewhat better than an adult's fingertip [3-5,9-12]. To enhance physical robustness and minimize the degree of electrical and mechanical coupling between discrete taxels, the PVDF film's upper surface served as a common low resistance electrical ground plane after it was uniformly coated with a sputtered nickel film (800 Å thick). The individual taxel electrodes (400 x 400 μm) were separated from their nearest neighbors by 300 μm.

The arrangement of the tactile sensor's amplification and output interface circuitry and the corresponding electrode matrix (without the PVDF film) is illustrated in Figure 1. The set of 64 *in situ* MOSFET amplifiers are located around the periphery of the taxel electrode matrix. Located at two of the IC's four corners are electrical ground pads which are used to establish a wire bond connection to the surface electrode (800 Å thick nickel film) on the PVDF film after it has been attached. The electrode matrix is surrounded by rectangular-shaped alignment marks to facilitate locating particular taxels which are masked after the PVDF film is attached. The pads on the IC's periphery are the wire bond pads used to interface the IC tactile sensor with a pin-grid array (PGA) package which served to facilitate load testing and the establishment of an interface with the externally configured multiplexer. To minimize stray surface leakage currents and parasitic coupling impedances, the level-one metal electrode interconnect conductors were electrically isolated with a 3-μm thick dielectric glass layer.

Relative to the ideal robotic tactile sensor characteristics discussed in the *Introduction*, the ideal force sensitivity threshold of the tactile sensor can be established by considering perpendicularly applied force components (neglecting the transverse stresses in the film plane). For this idealized situation, the charge sensitivity constant (S) for the 40-μm thick PVDF film utilized in this research can be interpreted as the axial piezoelectric stress constant (d_{33} = 16 x 10^{-12} coulombs/N) [19,20]. Thus, from Eqs. (1) and (2), for an applied force of 1 g (1 gmf) uniformly distributed over the 400 x 400 μm taxel electrode area, the open-circuit voltage (V) is expected to be approximately 0.41 V. In practice, however, this value will likely be smaller due to the inherent mechanical losses associated with coupling the applied load to the film, the presence of the adhesive used to attach the PVDF polymer to the taxel electrode matrix (manifests itself as a series capacitance), and the parasitic capacitance attributable to the electrode interconnect conductors.

To achieve a gain greater than unity for the *in situ* gate-coupled taxel amplifiers, a cascade configuration composed of two MOSFET inverting amplifiers was utilized. To ensure that the theoretically postulated 0.41-V open-circuit response associated with a 1 gmf load would not be seriously corrupted with noise when it is passed through the externally connected multiplexer circuit, the amplification stage was designed using SPICE® [22] to provide a gain of 1.25 in its linear operating region (2.5 to 13 V) which could be conveniently centered at 7.75-V for a 15-V (V_{dd}) operating bias.

As discussed in an earlier publication [20], a digital logic circuit was designed for this application to capture the tactile sensor's time-division multiplexed set of 64 amplified voltage responses within a 50 ms window. A digital storage oscilloscope (DSO) (Hewlett-Packard, Inc., model HP 54100A, Palo Alto, CA 94304) connected to the multiplexer's output facilitated the collection of this data stream; the synchronous output pulse generated by the digital logic circuitry [20] was used to trigger the DSO and expedite the collection of the tactile sensor's response. The overall data collection process was further automated with a microcomputer (Zenith Data Systems Corp., model Z-248, St. Joseph, MI 49085) equipped with an IEEE-488 interface plug-in card (Capital Equipment Corp., model 01000-60300, Burlington, MA 01730).

A critical feature of the tactile sensor's design was the inclusion of the PVDF film voltage bias pads (Figure 1) that were externally accessible after the PVDF film was attached to the IC. These pads were wire bonded to available IC package

pins which were correspondingly routed to the input terminals in an array of electrically-triggerable, ultra-low leakage (10^{12} Ω off-state) SPST CMOS IC switches (Maxim Integrated Products, model MAX327CPE, Sunnyvale, CA 94086). The output terminals of the switches were connected to the positive port of the 2.5-V power supply. The voltage bias pad which is connected to the metallized surface of the PVDF film was connected to the negative power supply terminal. When the switch was closed, it impressed the 2.5-V bias (V_{bias}) directly across the PVDF film. This capability was implemented to pre-charge and stabilize the PVDF film at the beginning of the taxel object imaging measurement cycle. Consistent with earlier reported results [20], pre-charge durations on the order of 0.1 seconds were experimentally found to yield an improved level of stability and response uniformity. A schematic of a discrete *in situ* taxel MOSFET amplifier design and pre-charge voltage bias arrangement is shown in Figure 2.

TACTILE SENSOR FABRICATION

The PVDF film (Solvay Technologies, Inc., SOLEF® product, New York, NY 10017 and Solvay & Cie, S.A., Brussels, Belgium) was attached to the IC using a urethane conformal coating (Miller Stephenson Chemical Company, coating MS-470/22, Danbury, CT 06810). A uniform 6-μm thick layer of the adhesive was deposited on the PVDF film square using a conventional photoresist spinner.

To ensure a uniform bond between the PVDF film and the IC, a teflon compression block and clamp was positioned to compress the (IC/urethane adhesive/PVDF film/compression block)-sandwich. Uniform contact between the PVDF film and the IC was facilitated by storing the sensor for 30 minutes in a vacuum chamber (10^{-6} Torr). Upon removal from the vacuum chamber, the entire assembly was cured in a 65 °C oven for 60 minutes. Finally, the uppermost metallized surface of the PVDF film was wire bonded to the IC's voltage bias pads.

TACTILE SENSOR PERFORMANCE

To minimize transient pyroelectric effects, the sensor's performance measurements were accomplished isothermally (22 ± 0.5 °C) under low-level illumination conditions (inside a dark-walled enclosure). The response of a discrete taxel upon the application of a 35-gmf load revealed that the average onset response time (load application) was approximately 0.04 seconds (25 Hz bandwidth), and the average discharge time (load removed) was approximately 0.05 seconds (20 Hz bandwidth). No significant variance was observed in these two parameters for loads spanning 0.8 to 135 gmf. The asymmetry observed between the response and discharge times suggests that the sensor possesses a slight degree of hysteresis.

The discrete taxel performance response of sensors fabricated with the 40-μm thick PVDF film and pre-charged (initialized) with the 2.5-V no-load bias were collected for 0.5 to 150 gmf loads that were uniformly applied to a set of six randomly selected electrodes. As depicted in Figure 3, the sensor manifested a linear response (0.07 V/gmf slope) for loads spanning 0.8 to 135 gmf.

To evaluate the viability of tactile object imaging, the pre-charge stabilization cycle was implemented to establish a uniform pre-load response condition for the 64 taxels [20]. The enhanced level of stability and response uniformity achieved with the pre-charge bias technique is illustrated in Figure 4. After the unloaded but pre-charged sensor matrix was scanned and the discrete taxel responses were transferred from the DSO to the computer, a load with a particular shape and weight was applied to the sensor. The external digital logic circuitry was utilized to scan the taxel matrix, the DSO captured the response of each MOSFET amplifier (stored as the arithmetic average of 8 measured values), and the entire set of 64 taxel measurements were collected in 50 ms. When this measurement cycle was completed, the applied load was removed, the pre-charge cycle was repeated, the matrix was scanned, and a post-load sensor response data file was created. The post-load voltage bias implementation served two purposes. In addition to its obvious importance as a sensor stability indicator, it was also utilized in the tactile object image interpretation investigation to form a compensated baseline no-load response matrix that was calculated by averaging the corresponding pre- and post-load taxel responses and then taking the absolute value of the result.

To generate a tactile object image, the values in the compensated sensor response baseline matrix were subtracted from the corresponding values in the response matrix produced by an applied load. The values in the resulting matrix were then normalized with respect to the magnitude of the largest value in the matrix, and a three-dimensional cubic-spline fitted surface plot was generated (the xy-plane corresponds to the taxel positions in the sensor matrix, and the z-axis maps the associated normalized response values). Table 1 describes the load shapes that were evaluated.

The following procedure was implemented to generate the tactile object image recognition criteria to assess the capability of the sensor to discern different object shapes applied with the same gmf load. The sharp-edge shaped load was selected as a fundamental shape, from whose response, criteria was established for recognizing the tactile object image generated by the other load shapes. As depicted in Figure 4, the sharp-edge shaped load could be readily positioned to contact a single row, column, or internal diagonal of the taxel matrix. The criteria of matching, as closely as possible, the actual surface contact area of the applied load and that bounded by a closed contour (parallel to the xy-plane) in the normalized three-dimensional response surface plot was implemented. For example, Figure 5 *a)* depicts the normalized three-dimensional response voltage plot produced by the 100 gmf sharp-edge load. Figure 5 *b)* depicts the z-axis value of 0.90 V that yielded the best-fit (contours examined at 0.01 V increments) for imaging the shape of the applied load.

To validate this rudimentary object image recognition criteria, the remaining load shapes (Table 1) were independently applied as 100 gmf loads, and the data was correspondingly processed. Figure 6 depicts the corresponding plots associated with a representative set of the more complex load shapes, and Table 2 summarizes the best-fit conditions identified for each particular shape. It is noted that the overall best-fit normalized voltage response value (z_{ave} = 0.91 V; std dev = 0.019 V) agrees reasonably well with the level identified for the sharp-edge shaped load. To assess the validity of this image recognition criteria for loads spanning the linear response range of the sensor (0.8 to 135 gmf), the measurement process was repeated for 10 and 50 gmf loads. The results associated with this segment of the performance evaluation are included in Table 2. While not absolutely precise, the trend associated with the data in Table 2 suggests that a fundamental shape, such as a sharp-edge, may be used to calibrate and establish the first-order criteria for generating the tactile object image of a load with a different shape.

By direct extension of the proposed tactile object imaging technique, the gmf of an arbitrary load (limited to the sensor's linear response region) can be correspondingly determined by using the characteristic best-fit normalized voltage threshold criteria (z_{ave} = 0.91 V) to identify those taxels which define the load's silhouette. By arithmetically averaging the pre-normalized voltage response values of the selected taxels, the equation of the linear least-squares sensor calibration line (Figure 3) can be solved to estimate the corresponding gmf value of the applied load.

CONCLUSION

The objective of this research was to design and evaluate the performance of a tactile sensor by mechanically and electrically coupling a 40-μm thick piezoelectric PVDF film to an IC containing an array of 64 high-input impedance MOSFET amplifiers. The historically persistent limitation of piezoelectric-based tactile sensors associated with response stability and reproducibility has been resolved via the successful implementation of the pre- and post-load voltage bias technique. The implementation of the initializing voltage bias technique also facilitated the development of a first-order pattern recognition processing scheme that can be used to establish the shape (resolution on the order of 700 μm) and approximate gmf of an applied load.

REFERENCES

1. Dario P. and de Rossi D., Tactile Sensors and the Gripping Challenge, *IEEE Spectrum*, **22**: 46-52, 1985.
2. Fielding P.J., Evaluation of a Robotic Tactile Sensing System, *Sensors*, **3**: 35-46, 1986.
3. Barth P.W., Sensor Applications in Robotics, *Robotics Engineering*, **8**: 195-218, 1986.
4. Regtien P.P.L., Sensors for Applications in Robotics, *Sensors and Actuators*, **10**: 195-218, 1986.
5. Regtien P.P.L., Sensor Systems for Robot Control, *Sensors and Actuators*, **17**: 91-101, 1989.
6. Rooks B., Tactile Sensing Should Not Be Forgotten, *Sensor Review*, **3**: 2, 1983.
7. Severwright J., Tactile Sensor Arrays - The Other Option, *Sensor Review*, **3**: 27-29, 1983.
8. Arbib M.A., Overton K.J. and Lawton D.T., Perceptual Systems for Robots, *Interdisciplinary Science Reviews*, **9**: 31-46, 1984.
9. Harmon L.D., A Sense of Touch Begins to Gather Momentum, *Sensor Review*, **1**: 82-88, 1981.
10. Harmon L.D., Tactile Sensing for Robotics, in *Robotics and Artificial Intelligence, NATO Adv. Study Inst. Series F: Computer and System Science, vol. 11*, Brady M., Gerhardt L.A. and Davidson H.F. (eds.), Springer-Verlag, Heidelberg, 1984.
11. Harmon L.D., Automated Tactile Sensing, *Int. J. Robotics Research*, **1**: 3-32, 1986.
12. Harmon L.D., Robotic Taction for Industrial Assembly, *Int. J. Robotics Research*, **3**: 72-76, 1983.
13. Giallorenzi T.G., Bucaro J.A., Dandridge A., Sigel G.H., Cole J.H., Rashleigh S.C. and Priest R.G., Optical Fiber Sensor Technology, *IEEE J. Quantum Electronics*, **QE-18**: 626-663, 1982.
14. Senturia S.D., The Role of the MOS Structure in Integrated Sensors, *Sensors and Actuators*, **4**: 507-526, 1983.
15. Voorthuygen J.A. and Bergveld P., The PRESSFET: An Integrated Electret-MOSFET Based Pressure Sensor, *Sensors and Actuators*, **14**: 507-526, 1983.
16. Hackwood S., Beni G., Hornak L.A., Wolfe R. and Nelson T.J., A Torque-Sensitive Tactile Sensor Array for Robotics, *Int. J. Robotics Res.*, **2**: 46-50, 1985.
17. Dario P., Bardelli R., de Rossi D., Wang L.R. and Pinotti P.C., Touch-Sensitive Polymer Skin Uses Piezoelectric Properties to Recognize the Orientation of Objects, *Sensor Review*, **2**: 194-198, 1982.
18. Lerch R., Electroacoustic Transducers Using Piezoelectric Polyvinylidene Films, *J. Acoust. Soc. Am.*, **66**: 952-954, 1979.
19. Gallantree H.R., Review of Transducer Applications of Polyvinylidene Fluoride, *IEE Proc.*, **130**: 219-224, 1983.
20. Kolesar, Jr. E.S., Reston R.R., Ford D.G. and Fitch, Jr. R.C., Multiplexed Piezoelectric Polymer Tactile Sensor, *J. Robotic Systems*, **9**: 37-63, 1992.
21. *MOSIS - Metal Oxide Semiconductor Implementation Service User's Manual.* Information Science Institute, University of Southern California (USC/ISI), Marina del Rey, CA, release 3.0, 1988.
22. Antognetti P. and Massobrio G., *Semiconductor Device Modelling with SPICE.* McGraw-Hill, New York, NY, 1988.

TABLE 1. DESCRIPTION OF THE LOAD SHAPES USED TO EVALUATE THE OBJECT IMAGING PERFORMANCE OF THE TACTILE SENSOR

Load Shape	Dimensions (mm)
Sharp Edge	5.8 (length) x 0.7 (width)
Square	2.8 (edge length)
Trapezoid	4.2 (base) x 2.7 (altitude) x 1.5 (altitude)
Isosceles Triangle	3.7 (base) x 3.8 (altitude)
Small Circle	2.7 (diameter)
Large Circle	4.2 (diameter)
Toroid	4.6 (outer diameter) x 1.8 (inner diameter)
Slotted Screw	4.8 (diameter) x 0.7 (slot width)
Cross-Slotted Screw	4.8 (diameter) x 0.7 (slot width)

TABLE 2. NORMALIZED VOLTAGE RESPONSE BEST-FIT VALUES FOR THE LOAD SHAPES

	Applied Load		
Load Shape	10 (gmf)	50 (gmf)	100 (gmf)
Sharp Edge	0.93 V	0.91 V	0.90 V
Square	0.88 V	0.90 V	0.91 V
Trapezoid	0.92 V	0.93 V	0.89 V
Isosceles Triangle	0.88 V	0.90 V	0.89 V
Small Circle	0.95 V	0.94 V	0.92 V
Large Circle	0.92 V	0.93 V	0.91 V
Toroid	0.95 V	0.90 V	0.92 V
Slotted Screw	0.92 V	0.91 V	0.91 V
Cross-Slotted Screw	0.91 V	0.90 V	0.88 V

(Average = 0.91 V; Standard Deviation = 0.019 V)

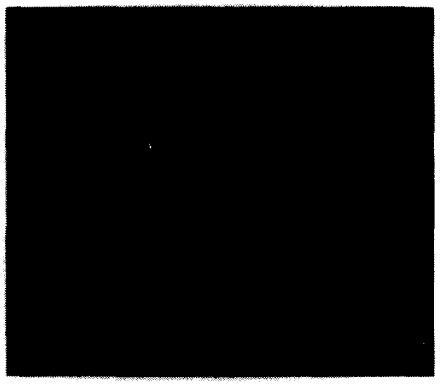

Figure 1. Photomicrograph of the silicon IC tactile sensor with peripheral dimensions of 9200 x 9200 μm (without the piezoelectric PVDF film).

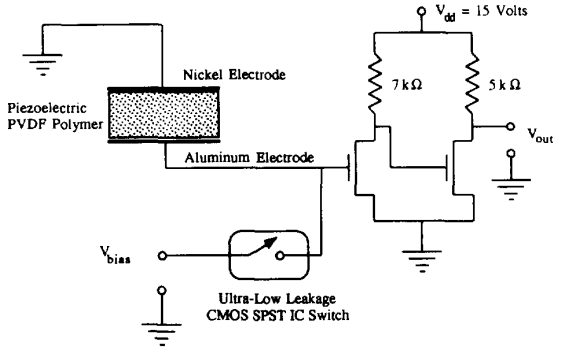

Figure 2. Schematic of a discrete *in situ* MOSFET amplifier and electrically-triggerable, ultra-low leakage (10^{12} Ω off-state) SPST CMOS IC switch configuration used to pre-charge each taxel.

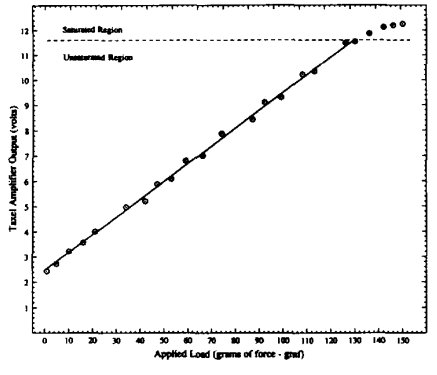

Figure 3. Discrete taxel response for loads uniformly applied to the area of the PVDF film's lower electrode. (Each data point represents the arithmetic average of six independent measurements; the equation of the linear least-squares line is: $V_{response}$ = (0.07 V/gmf)(Applied load in gmf) + 2.5 V; the 2.5 V pre-charge bias was applied before each load measurement).

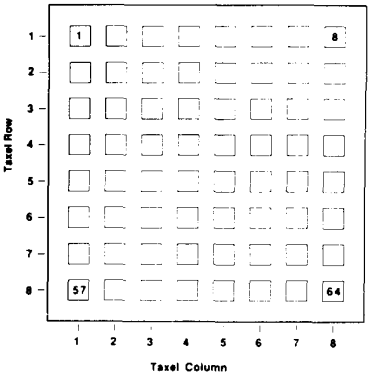

(a)

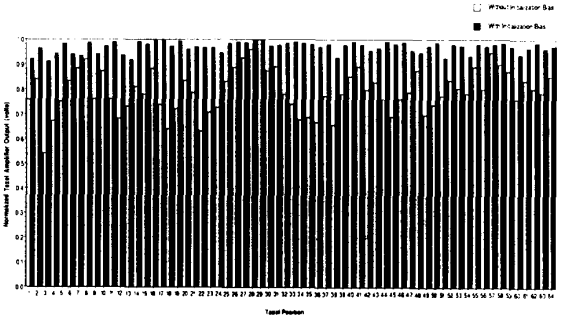

(b)

Figure 4. Utility of the pre-charge (stabilization) bias cycle that is applied to the PVDF film. *(a)* Taxel electrode position identification scheme. *(b)* Multiplexed sensor response of the unloaded 8 x 8 taxel matrix before the pre-charge bias was applied to the PVDF film compared to the improved (stabilized) state of the same unloaded sensor after the short duration pre-charge cycle was accomplished (2.5-V bias applied for 0.1 seconds).

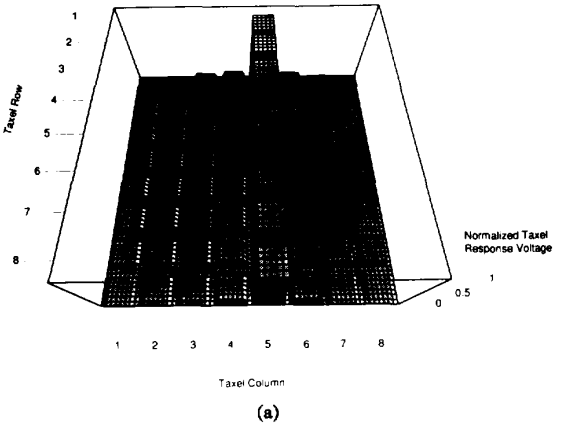

(a)

Figure 5. Multiplexed tactile sensor response resulting from the application of the 100 gmf sharp-edge shaped load. *(a)* Three-dimensional plot of the normalized voltage response (z-axis) versus position in the 8 x 8 taxel matrix (xy-plane) when the load was applied to a column of taxels. *(b)* Corresponding overlay of the sharp-edge shaped load (shaded rectangle) relative to the normalized voltage response best-fit level (z = 0.90 V); the darkened taxels are those whose normalized response was greater than or equal to the threshold value. *(c)* Three-dimensional plot of the 100 gmf sharp-edge shaped load applied to an internal diagonal of taxels. *(d)* Corresponding overlay of the sharp-edge shaped load.

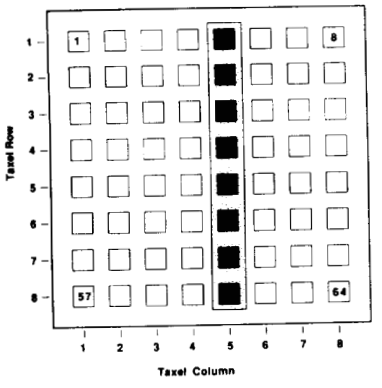

(b)

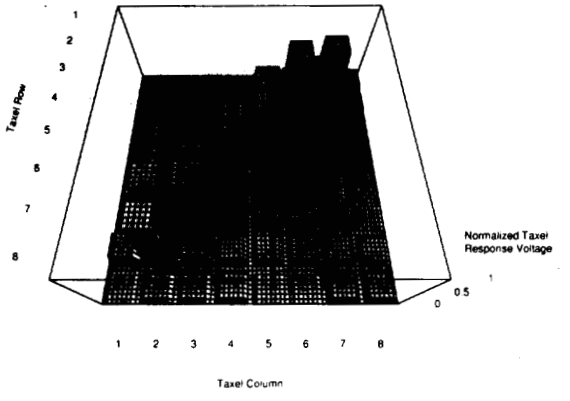

(c)

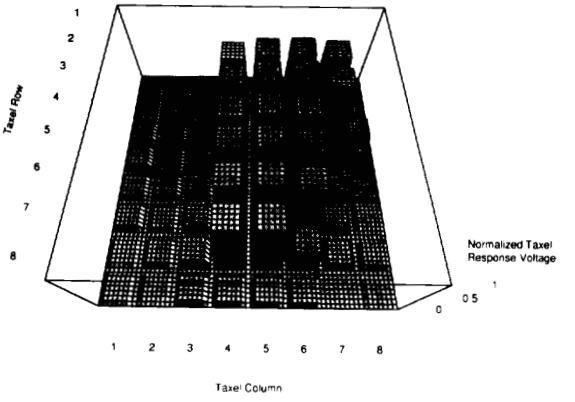

(a)

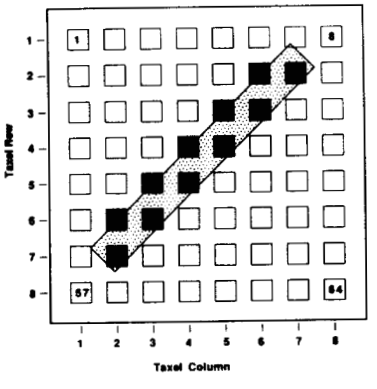

(d)

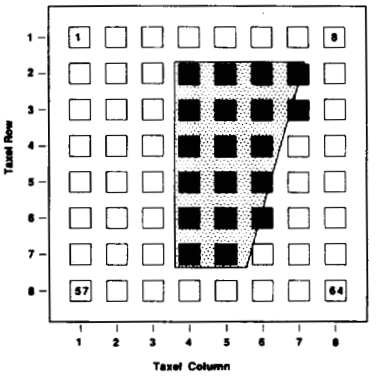

(b)

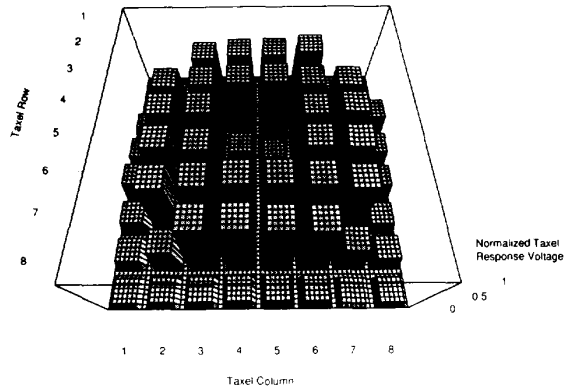

(c)

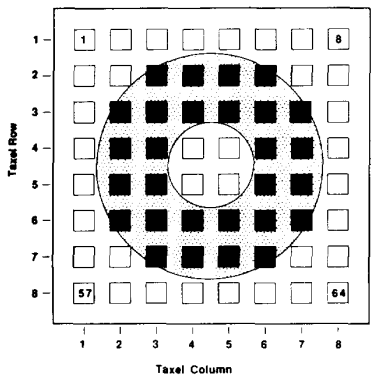

(d)

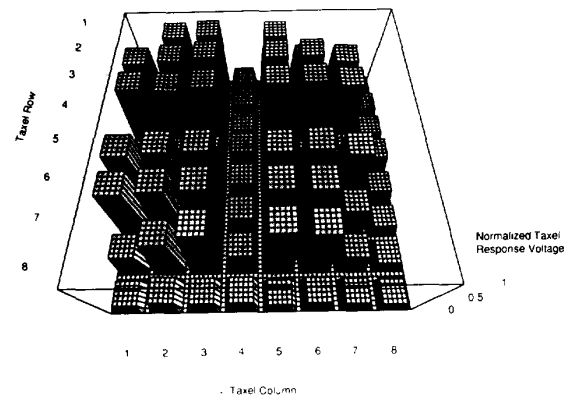

(e)

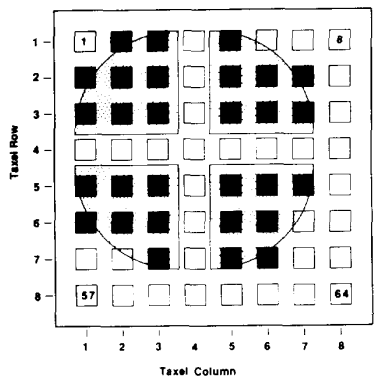

(f)

Figure 6. Multiplexed tactile sensor response resulting from the application of several 100 gmf load shapes. *(a)* Three-dimensional plot of the normalized voltage response (z-axis) for the trapezoid load versus position in the 8 x 8 taxel matrix (xy-plane). *(b)* Corresponding overlay of the trapezoid shaped load (shaded rectangle) relative to the normalized voltage response best-fit level (z = 0.92 V); the darkened taxels are those whose normalized response was greater than or equal to the threshold value. *(c)* Three-dimensional plot of the normalized voltage response for the toroid load versus position in the 8 x 8 taxel matrix. *(d)* Corresponding overlay of the toroid (shaded region) relative to the normalized voltage response best-fit level (z = 0.92 V); the darkened taxels are those whose normalized response was greater than or equal to the threshold value. *(e)* Three-dimensional plot of the normalized voltage response for the cross-slotted screw load versus position in the 8 x 8 taxel matrix. *(f)* Corresponding overlay of the cross-slotted screw (shaded regions) relative to the normalized voltage response best-fit level (z = 0.88 V); the darkened taxels are those whose normalized response was greater than or equal to the threshold value.